Investigation of Vacuum Arc Droplets from Copper, Titanium, and Tungsten by Means of Light Scattering

Peter Siemroth, Michael Laux, Heinz Pursch, Jürgen Sachtleben, Martin Balden, Volker Rohde, Rudolf Neu

***Abstract*—Studies of molten droplets emitted from cathode spots of vacuum arcs on copper, tungsten, and titanium have been carried out using a time-of-flight measurement procedure. In the arrangement two light barriers at different distances from the cathode surface are used. When particles traverse the barriers, the appearance of scattered light can be used to establish the flight time and, thereby, the velocity of particles. Simultaneously, the intensity of scattered light provides a measure of the size of the particle by applying the Mie-scattering theory together with calibrations. By turning the cathode surface with respect to the drift tube axis, an angular resolution of the parameters was achieved. Algorithms were developed for automated processing of the measured data to identify particles arriving from the arc spot unobstructed. Distributions of the particle sizes, a statistical relation between the sizes and the emission velocities of particles, and other properties are discovered for all three cathode materials.**

***Index Terms*—Vacuum arc, cathode spot, light scattering, droplet velocities, droplet sizes.**

I. Introduction

DURING the existence of a vacuum arc, cathode spots emit material in the form of plasma, neutral vapor, and molten particles. The share of molten particles depends on the cathode material and ranges from 3.5% of the eroded material for tungsten to 90% for lead [1].

In many investigations, the analysis of the size was based on particles deposited on collectors and afterwards individually characterized by optical or scanning electron microscopy. In some experiments, the collectors were used as parts of a rotating drum arrangement acting as a velocity filter [2]. Applying the collector technique, droplet sizes from several nm to 100 µm were identified and velocities from a few to about 100 m/s were observed. Much of the previous work dealt with either sizes or velocities of arc particles. However, photographic observations have shown that particles are easily bounced from solid components before getting caught. Hence, the observed sizes and velocities are flawed, and their distributions are distorted. The distributions were measured more comprehensively by scattered laser light (Laser Doppler Anemometry [3]) and further information was also revealed by the application of high-speed cameras [4]. Beyond that, the experimental parameters differ regarding arc currents (pulsed arcs, DC arcs, or high current arcs) and discharge durations (e.g., [5]-[11]).

The understanding of the particle emission from the arc spot and their interaction with the surrounding plasma is important in terms of some technical applications and problems in other research fields. The influence of particles became apparent by using vacuum arc deposition systems for thin-film production. The quality of coatings is deteriorated by failures and defects due to particles attached or embedded during the generation of films (e.g., [9], [12], [13]).

Characteristic arc tracks and attached particles were also found on parts of plasma-facing components (PFCs) of fusion devices. For example, a growing interest in data of the particle emission from refractory metals has emerged (e.g., [14], [15]), because tungsten is a favorite material for PFCs of future reactors like ITER. An in-depth analysis of the consequences of arc erosion on plasma-facing materials in large fusion devices demonstrates that their occurrence can be a significant source of impurities in the plasma, because under certain conditions (size, velocity, temperature, emission direction), molten particles produced by arcing may pass the edge region of the machine and evaporate in the core plasma [14].

Additionally, such data are helpful for the basic physics of the cathodic processes of vacuum arcs and, especially, the verification of specific aspects of the modelling of the particle emission from the cathode spot (e.g., [16], [17], [18]).

In this study, results of new measurements of particle ejection from copper (Cu), tungsten (W), and titanium (Ti) cathodes are presented as a continuation and extension of former work [19] restricted to Cu. Particularly, results of a simultaneous measurement of the size and the flying speed of the individual particle are reported. The diameters as well as the velocities are determined for undisturbed free-flying particles, resulting in more precise and more reliable values, and the whole range of emission directions is covered. In addition, distributions for the whole droplet ensemble are given as well.

II. Experimental

The used setup has been described in detail elsewhere [19]. Arcs carrying 500 A for 1 ms are burned in a vacuum chamber (pressure 10^{-5} Pa) consisting of a cathode compartment connected to a drift-tube. The cathodic section includes a

Manuscript received December 28, 2021.

Peter Siemroth, Michael Laux, Heinz Pursch and Jürgen Sachtleben were with the Arc Precision GmbH, (retired employees), Scheederstrasse 29a, 15711 Königs Wusterhausen, Germany. (email: info@arcprecision.com).

Martin Balden, Volker Rohde and Rudolf Neu are with the Max-Planck-Institut für Plasmaphysik, Boltzmannstrasse 2, 85748 Garching, Germany. Rudolf Neu is also with the Technische Universität München, Boltzmann-strasse 15, 85748 Garching, Germany.

rotatable unit holding an exchangeable cathode plate (50 x 60 x 10 mm³) made of Cu, W, or Ti, together with an ignition electrode. To change the orientation of the cathode, the whole vessel is vented and the cathode-unit rotated by a pre-selected angle α between 0° and 90°. The drift-tube, equipped with two light barriers at two different distances to the cathode plain (432 mm and 679 mm, respectively), can be accessed by the ejected particles via a quadratic aperture (10×10 mm^2). Each light barrier contains a lamp emitting white light, a photo multiplier, and two optical systems to form the illumination beam and to image scattered light onto the multiplier, respectively. The observed volume, a 20×20×20 mm^3 cube, is smaller than the cross-section of the drift-tube.

Particles are emitted from the cathode spot that moves away from the ignition point by a random walk extending between 10 mm and 20 mm during the 1 ms of the discharge. If the ballistic track of particles emitted from the cathode spot is compatible with the direction given by the axis of the drift-tube, they may pass the aperture and then have a high probability to be detected in either one or two of the barriers. Many particles hit the roof at the end of the drift-tube and are reflected. On their descent, they may pass the barriers again. There is a certain probability that particles undergo small-angle collisions with the inner surface of the drift-tube. The arrival time of a particle at a barrier and its passing duration are closely connected, and they are functions of the emission velocity and the time of emission during the discharge.

III. DATA EVALUATION

A. Peak identification and characterization

The treatment of a time series of the intensity of the scattered light represented by photo multiplier voltages comprises two different essential tasks. Firstly, the robust elimination of disturbing pick-up signals and an effective reduction of noise stemming from the lamps, introduced by possible stray radiation, and photonic noise. Secondly, the identification of the peaks of scattered light originating from particles emitted by the cathode and passing the light barrier. A package of successive algorithms is applied to both signal channels (belonging to the lower and upper barriers) separately. A detailed description of the procedures is given in [20].

Pick-up signals (including a constant background) are detected by exploiting the data measured prior to the trigger of the discharge and subtracted from the entire time series. The remaining noise is treated by sliding window techniques in two steps. The first one is an extended median algorithm using time-windows of constant width to smoothen and reduce the number of data points. As a second step of the identification of peaks, windows having a temporal width that rises during time were applied to average the data. Unfortunately, the single peaks caused by passing particles lack a typical shape and, therefore, they are difficult to distinguish from larger noise-peaks shortly after the end of the discharge, because the peak-width expected from the ballistics is comparable to that of typical noise then. As a consequence of the application of time dependent averaging windows, the remaining noise depends on time as well, and a constant threshold to discriminate peak regions has to be replaced by a curve of thresholds depending on time. Fitting a hyperbolic time dependence to the data gives a first approximation for the threshold-curve enabling a first exclusion of regions belonging to the largest peaks. On the one hand regions of possible peaks are identified, on the other hand omitting those regions improves the background data by clearing it from peak contributions. Repeating the procedure a few times leads to a quite complete list of selected peaks.

As the extracted peak regions are still modulated by noise, a compaction is added to enclose possible side parts of the peak. Finally, every possible peak is characterized by several parameters (compare Fig. 2 in [20]) used to validate the peak in the framework of predetermined criteria. An approximate emission velocity of the particle results from the time of appearance of the peak, whereas the peak height is used to determine the particle size exploiting a calibration (see chapter C).

B. Identification of particles

The temporal width of the peak is cross-checked against the duration of the passage given by ballistics to validate the peak. In case the same particle appears in both light barriers, the result for the velocity can be improved further and, additionally, the time of emission during the discharge can be determined.

Fig. 1 shows an oscillogram containing a succession of two peaks in the upper channel escorted by two peaks in the lower one. In case the first low-up pair belongs to the same particle, it can be hypothesized that the follow-up pair is caused by the very same particle after a reflection at the roof of the vacuum vessel. The impact time expected for the rising particle and the start time for the descent from the roof can be cross-checked. If the two times fit for such a chain of events, the collision time at the roof and the velocity loss during the collision can be calculated assuming that the particle does not disintegrate during the impact.

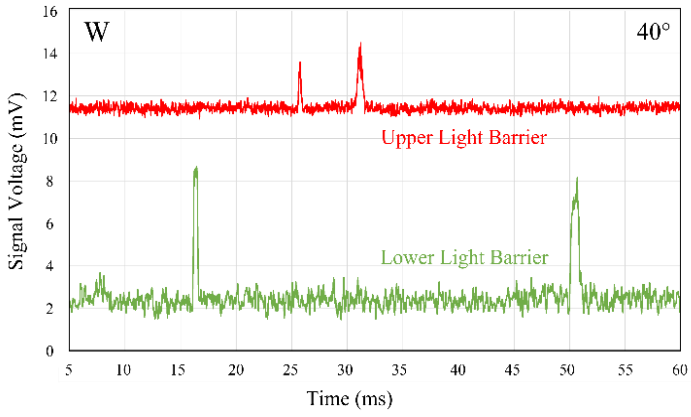

Fig. 1. Cutout of an oscillogram of the signals for the lower and upper light barriers presumably produced by rise and fall of the same particle (sampling of 10.4 MS/s at 14-bit resolution, presentation digitally smoothed with a bandwidth of 8kHz and 3 kHz for the upper and lower channel, respectively).

C. Calibration

The calibration, i.e., the determination of the relation between the multiplier voltage signal and the diameter of the corresponding particle scattering the light was a multistep process. From the Mie-theory it is well known that the intensity distributions have complex scattering structures due to resonance and interference effects, especially if the diameter of the particle and the wavelength of the scattered light are close to each other. To flatten those structures out, we used white light from a discharge lamp covering a wide range of wavelengths. Ab-initio Mie-scattering simulations confirmed that there is a bijective relation between the amount of scattered light and the droplet dimension. For particles with diameters larger than 1 µm, we found a nearly linear dependence between intensity and the square root of the diameter [19].

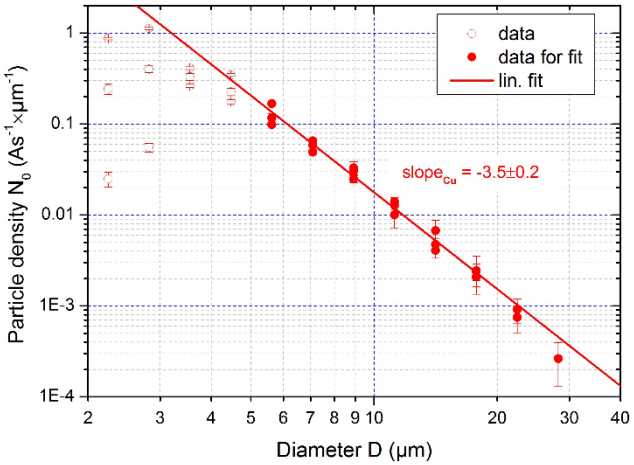

Fig. 2. Number of droplets seen in the field of view summed up for all angles and normalized to the time integrated discharge current (particle density) depending on the mean diameter for Cu. A linear fit was carried out for all full circles.

Using the spectral emission data of the lamps the efficiency of our optical system, and the luminous sensitivity of the multipliers together with the results from the Mie-calculations, we got a first estimate of the signal/diameter-function. In addition, the calibrated set-up was used to carry out scattering experiments with steel balls as test particles. The smallest test ball had a diameter of 0.4 mm. In this way, we got precise data, even though the test particles were about a hundred times larger than the droplets expected.

Due to the fact that the properties of the lamps, the multipliers, and the optics are fixed for all experiments, we can use the Mie-results to extend dependences established for Cu to other metals. In a final step, we compared the distributions obtained with experimental data published by Daalder [2]. The comparison of the scattering signals from droplets flying through both channels provided a final improvement of the calibration. Ultimately, a set of values for the proportionality factor A in the calibration formula

$$D = A \cdot \sqrt{U_{max}} \tag{1}$$

(with D the droplet diameter in µm and U_{max} the peak voltage in mV taken from the oscillogram) was found.

IV. Results and Discussion

A. Size Distribution

Generally, the size distribution is given by the number of particles detected in a pre-selected tight angular section and a narrow range of diameters as a function of this diameter. Even though the restriction for the angle results in poor statistics, all distributions constructed for a certain angular range follow power laws showing comparable negative exponents, albeit their pre-factors differ. Utilizing this feature, the distribution functions for the different angles can be fitted using a power law having a common exponent to get a new set of pre-factors. Therefore, it can be suspected tentatively that the distribution of particle diameters is independent of the emission angle and can be improved by merging the diameters for all angles. This assumption requires that the process determining the particle size is independent of the mechanism fixing the direction of ejection.

Fig. 2 shows the particle density, namely the frequency of occurrence of droplets per size class and integral current as a function of the mean diameter following a power law

$$\frac{dN}{Q \cdot dD} = N_0(\alpha) \cdot \left({}^{D}/_{D_0}\right)^{p} \tag{2}$$

with N_0 the droplet number for a given angle α, normalized to the charge, Q the time integrated current of all discharges, D the diameter of the droplets, D_0 = 1.0 µm, and p the slope of the fit-function.

The improved statistics covering all experimental conditions and angles gave p = -3.5 ± 0.2 (close to the former result in [19]). Similar dependences were measured for various cathode

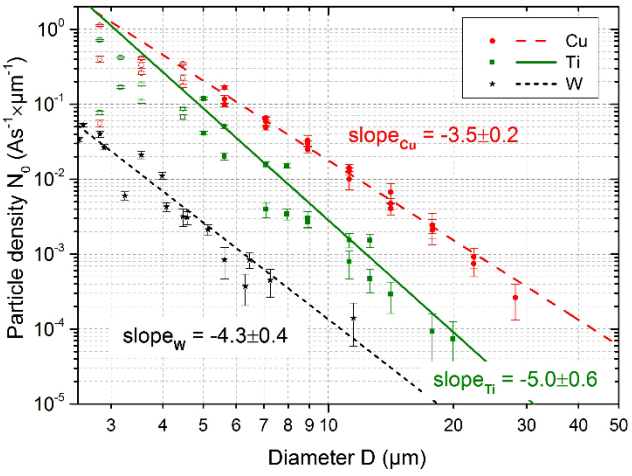

Fig. 3. Number of all individual particles registered in both channels per size class and per time integrated current within the field of view of the light barriers (shown for Cu, Ti, and W) following power laws.

materials and different arc conditions (e.g., [1], pages 269-277). In all studies for Cu, the obtained size distributions follow power laws with exponents between -2.5 and -3.5.

In the same manner as for Cu the size statistics for Ti and W are studied. The results are similar, namely, numbers of droplets fall with rising diameters following a power law (Fig. 3), although the exponents are different for the different metals. A power law extending over a large range of diameters can be considered as a support for the fractal nature of cathode spot processes [1]. Principally, the droplet numbers are the highest with Cu, they are somewhat lower with Ti, and much lower with W.

B. Angular Distribution

The number of emitted droplets at a given emission angle was determined as the number of droplets hitting a defined area (the cross-section of the light barrier) at a given distance (the height of the light barrier above the cathode) flying in a specific direction (determined by the inclination of the cathode). This amount can be estimated from the pre-factors N_0 of the distributions of droplet-sizes now carried out for the different angular ranges individually.

The procedure implies the independence of the angular distribution on the selected diameter of the particles. Taking into consideration, that the drift-tube covers only a part of the overall range of solid angles having the same inclination with respect to the cathode, the particle numbers have to be corrected by the ratio of the full solid angle to the solid angle of the detection area. The resulting angular distribution of the particle density shown in Fig. 4 can be represented by a simple polynomial of 3rd degree in the angle. Integrating this polynomial fit-function up to a given angle provides the share of all angles below this one in the particle density (Fig. 4).

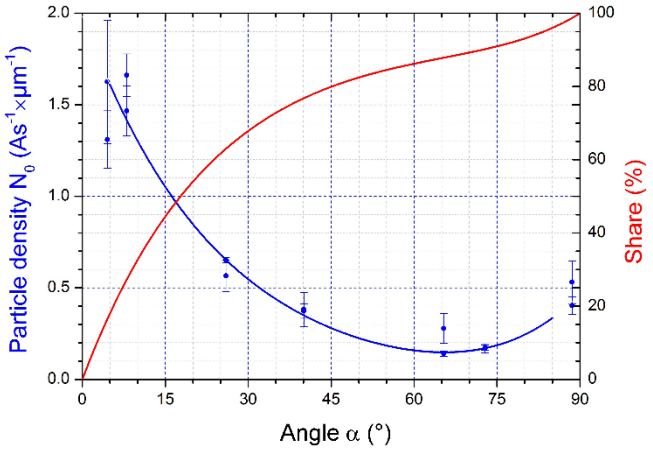

Fig. 4. Density of particles in relation to the emitting angle. Blue line: relative droplet number N_0 (comp. (2)) observed within the field of view.
Red line: percentage of all droplets (share in %), emitted at angles below certain value and converted to the full hemisphere.

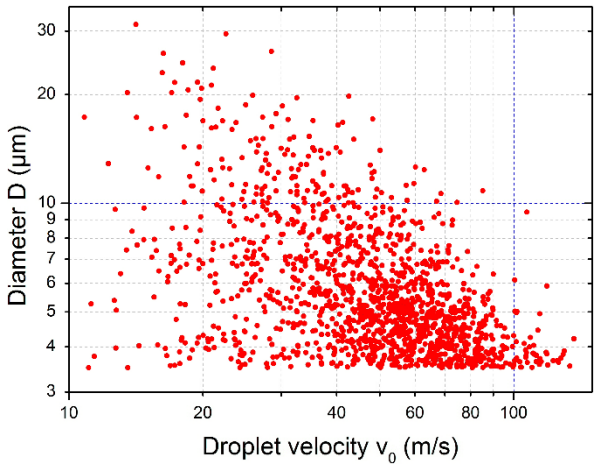

Fig. 5. Diameter vs. velocity plot for all Cu droplets, emitted under shallow angles (from 5° to 45°). The pairs of diameters and velocities for each confirmed peak are represented by one red dot.

C. Velocity vs. Size Distribution

The work reported here establishes a relationship between the sizes and velocities of individual droplets. Comparing the data from runs with different angles, it could be suspected that the distributions at angles below or above about 45° are quite different. Therefore, we studied the results for low (< 45°) and high (> 45°) angles separately.

1) Cu-Cathode Under Shallow Angles

Fig. 5 shows the velocities of all observed and verified droplets as a function of their diameters. Each of the red dots represents one Cu particle emitted under a shallow angle (from 5° to 45°), registered at least in one channel and verified based on their peak width and amplitude. Only peaks with an amplitude larger than a threshold value (corresponding to the noise level) are accepted. Such a threshold implies a lower limit of about 3.5 µm for the verified particles.

To get more valid statistics, the frequency of velocities was measured within a selected interval of diameters, starting with the small group containing the largest diameters (32 µm ≥ D > 13 µm), down to the smallest ones (4 µm ≥ D > 3.5 µm). As an example, in Fig. 6 the frequency distributions of the velocity for the three ranges with the largest mean diameters are given for Cu. All distributions could be successfully fitted by Gaussians. The integral over the Gaussian is equal to the number of considered peaks in that group. Generally, these numbers are different for the different groups.

In Fig. 7 only the Gaussian fits are shown but for all ranges of diameters of the Cu droplets. A normalization to the same number of particles in the diameter groups was carried out to make a comparison of the Gaussian distributions for different groups possible. It seems obvious that both, the mean velocities $\langle v_0 \rangle$ and the widths σ_v of the fitted velocity distributions increase for decreasing droplet sizes, whereas the relative width (i.e., $\sigma_v/\langle v_0 \rangle$) stays unchanged.

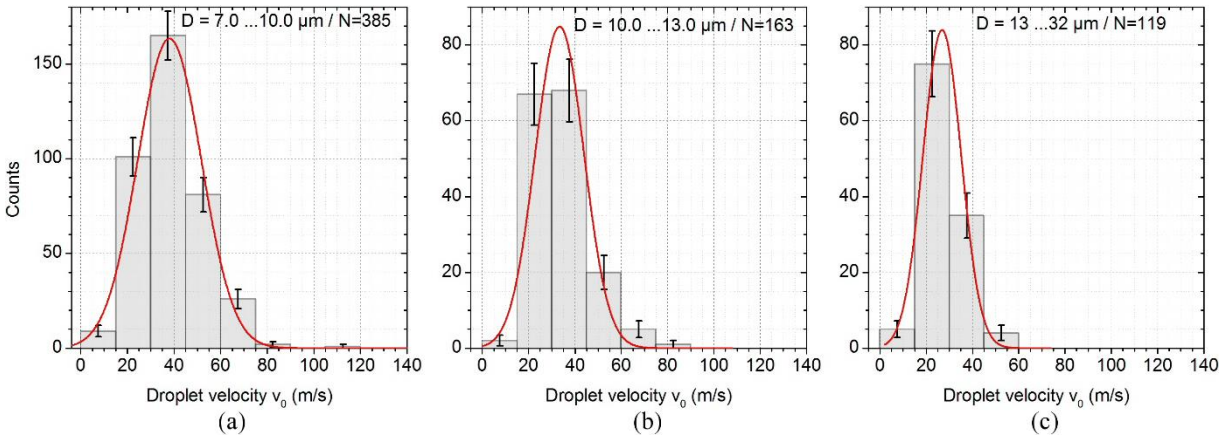

Fig. 6. Frequency distribution of the velocity given for the three largest diameter ranges (out of seven) of Cu droplets emitted at shallow angles together with the corresponding Gaussian fit curves.

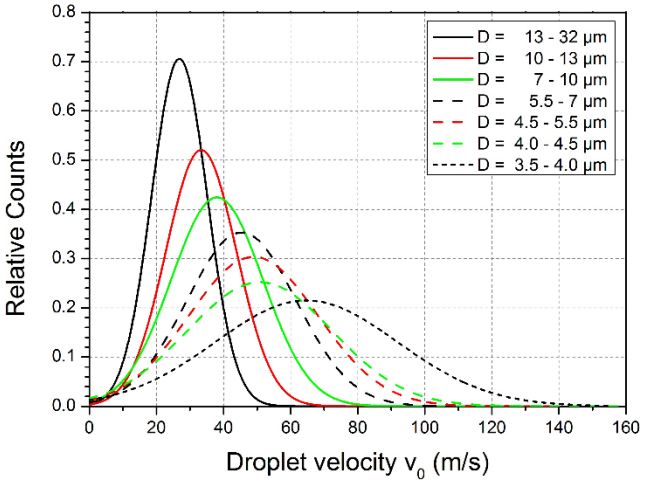

Fig. 7. Gaussians fit curves for the velocity frequencies of all diameter groups (Cu droplets).

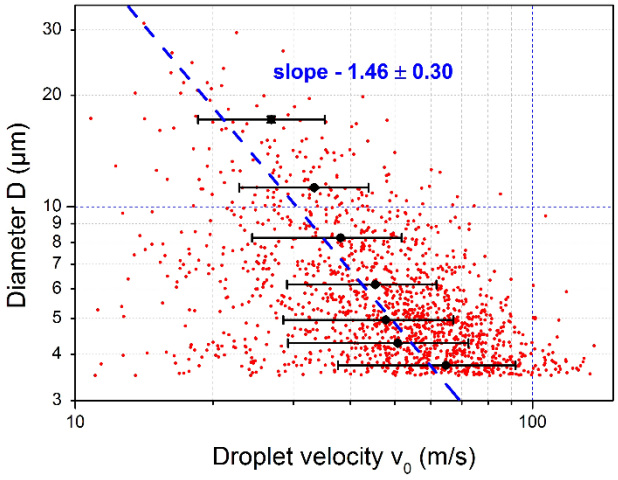

Fig. 8. Scatterplot of diameters D vs. velocities v_0 of Cu droplets together with the mean values $\langle v_0 \rangle$ and the widths Δv of the normalized Gaussian fits. The blue dashed line represents the best linear fit for a power dependence between diameter and velocity.

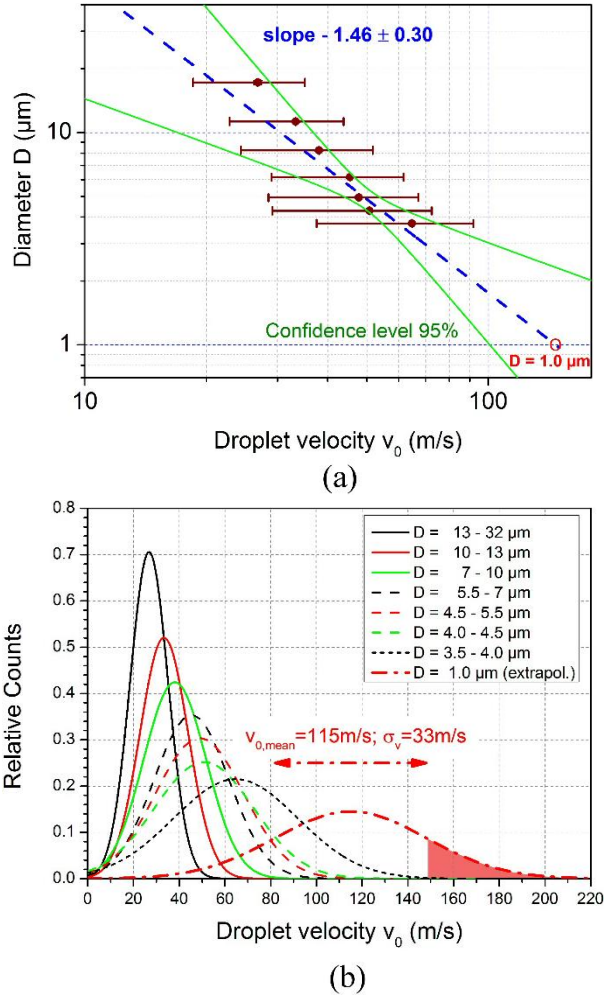

Fig. 9. Extrapolation of dependences to smaller diameters (Cu droplets).
(a) Extrapolation to a diameter of 1.0 µm together with the corresponding confidence range. The green lines indicate the corresponding confidence range. The extrapolation to smaller diameters, e.g., 1 µm (marked) is possible.
(b) Extrapolated Gaussian curve with the relative share of particles with a velocity deviation of more than 1σ (corresponding to velocities exceeding 140 m/s).

The numerous pairs of particle diameter and emission velocity for Cu are scattered over a zone reaching from 3.5 µm to 60 µm and from 10 m/s to 150 m/s. This large scatter is not adequately explained, even when accounting for the various sources of noise (electronic pick-up, photonic noise) and taking into consideration typical systematic errors characterizing the method of measurement (small angle collisions on the path, non-spherical particles). It can be stated that possible relations between the particle size and velocity are presumably of statistical nature. As expected, this statement extends to Ti and W. In Fig. 8 the mean velocities and the widths of the normalized Gaussian fits are added to the scatterplot of the data already shown in Fig. 5. A distinct dependence of the mean velocity on the diameter is found that can be described by $\langle v_0 \rangle \sim D^{-1.46}$.

In Fig. 9 (a) the fitted dependence is shown together with the confidence range of the fit and a conservative extrapolation to a diameter of 1 µm is carried out. The related Gaussian curve demonstrates the possible appearance of velocities exceeding 100 m/s (Fig. 9 (b)). Consequently, a 16%-fraction (> 1σ) may have even higher velocities, presumably beyond 140 m/s.

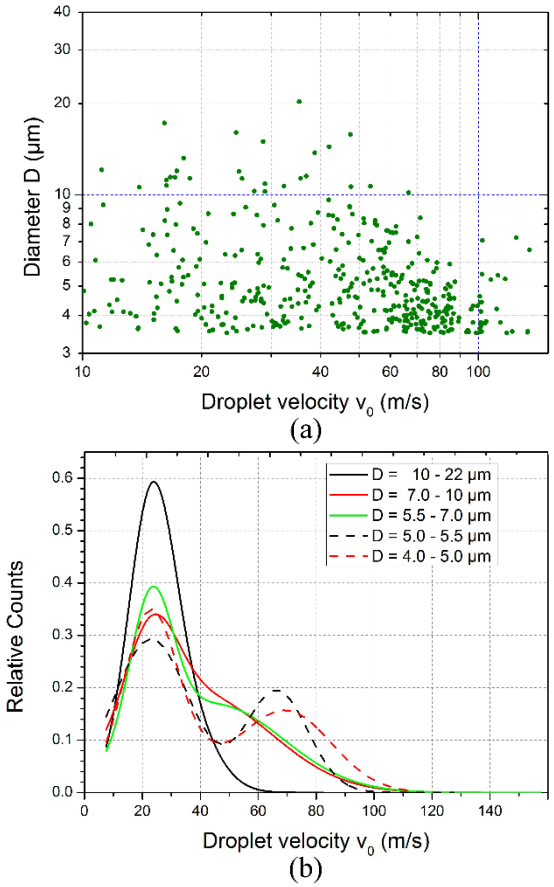

Fig. 10. Diameter vs. velocity plot for all Cu droplets, emitted under steep angles (from 45° to 90°).
(a) Scatterplot, each confirmed peak is represented by a green dot.
(b) Gaussians fit curves for the velocity frequencies of all diameter groups.

2) Cu-Cathode Under Steep Angles

For steep angles (45° to 90°) the scatterplot (Fig. 10 (a), comprising verified droplet peaks only) looks quite different as compared to the shallow angle case shown in Fig. 5. Two ranges of dots can be distinguished instead of grouping around a common mean value. The frequencies of velocities counted within intervals of diameters drawn against the velocity show always two maxima and, therefore, the best fit is always a double-Gaussian (examples are presented in Fig. 10 (b)).
Hence, the two groups of droplets are characterized by different velocities. Slow particles have about 20 m/s to 25 m/s, and a group of faster particles has about 60 m/s to 80 m/s. Surprisingly, no clear dependence between the mean velocities and the diameters for either of these two groups could be found. There is a slight tendency for larger droplets to presumably belong to the slow group, whereas smaller particles tend to belong to the faster group.

3) Ti- and W-Cathodes

For Ti and W, the velocity vs. size distribution was studied in the same manner. In both cases, the statistics for particles emitted under steep angles was too poor for a detailed analysis, but two groups of particles can also be suspected. For shallow angles the behavior was like that of Cu. Presumably, the inclinations of the velocity vs. size-dependences were the same for all metals (within the limits of accuracy). For a given

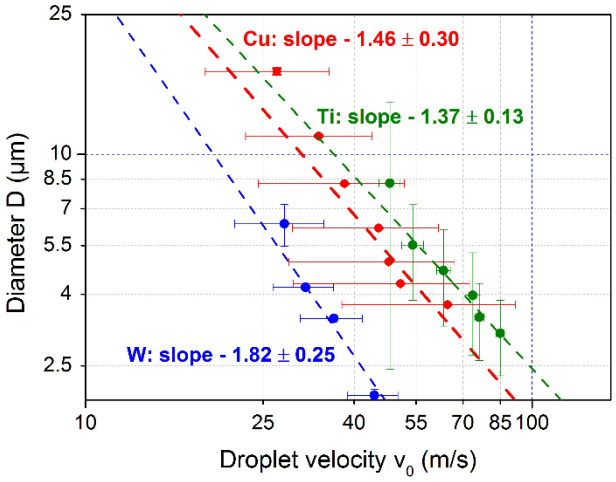

Fig. 11. Velocity vs. size distributions for all metals studied.

diameter, the velocity of Ti droplets is the highest, the velocity of Cu particles is somewhat smaller, and for W it is even about 50% smaller (Fig. 11).

D. Reflection of Particles at the Roof Flange

In a realistic environment like a coating unit or the edge of a magnetic fusion device, the path of a flying particle is often interrupted by a collision with parts of the solid structure. The circumstances of the collision (sticking probability, adhesion

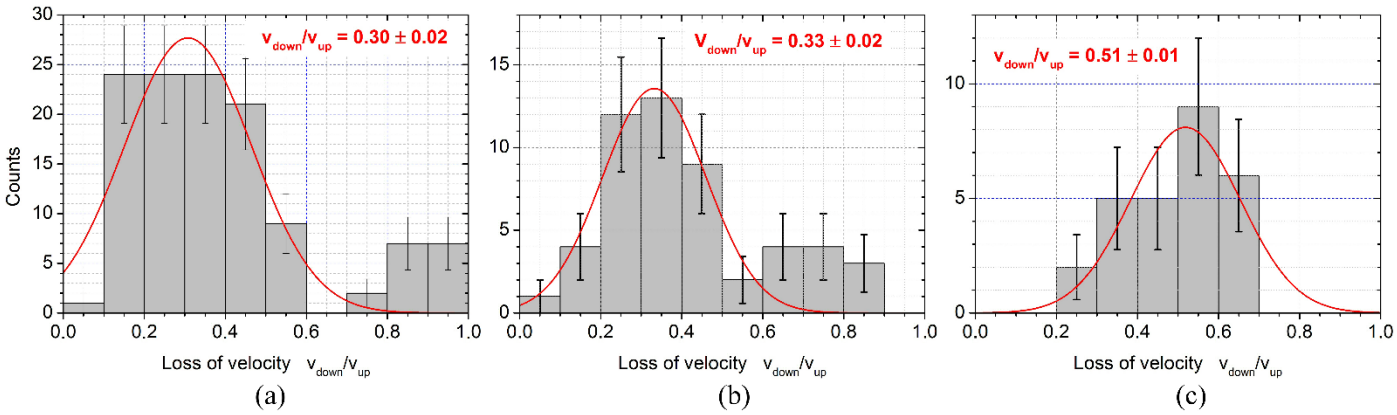

Fig. 12. Velocity loss due to reflection at the roof flange described by the ratios of the velocities after and before contact (a) Number frequency and Gaussian fit for Cu droplets. (b) for Ti droplets. (c) for W droplets.

times, ductile deformation, momentum loss) strongly determine the continuation of the particle's path. Due to the geometry of the drift-tube as a main part of the vessel many of the emitted particles underwent weak collisions under shallow angles with the tube wall. These undesired reflections prohibit a valid interpretation in terms of emitting velocity. Therefore, the related peaks were rejected by the verification process. Furthermore, a particle passing the whole drift-tube will unavoidably suffer an almost upright collision with the roof flange.

In the cases of an instantaneous reflection followed by a free fall registered by two more verified peaks (in the upper and lower channel, respectively) a reflection at the roof flange can be investigated in detail. Assuming, that the reflection takes place without disintegration, the velocity loss can be determined. It was found that reflected particles retrieve only a small part of their impact velocity. In the case of Cu, the reflected velocity amounts to about 30% of the impinging one, for Ti about 33%, and for W about 51% (Fig. 12).

V. SUMMERY AND CONCLUSION

The applied measuring technique combining a time-of-flight arrangement and the recording of the scattered light was successful in determining the size and velocity of particles emitted from the spots of arc cathodes. Analyzing the optical setup, carrying out extensive Mie-calculations, making calibration experiments with metallic test balls, and comparing the results with other published data, a reliable calibration of the measured multiplier voltage in terms of particle diameters has been established. From the statistical evaluation of experimental data, the following conclusions can be drawn:

- The arrangement can identify particles with diameters larger than 3.5 µm having typical emission velocities from about 10 m/s to 100 m/s.
- The distribution of particle diameters suggests decoupled dependences on diameter D and emission angle α, respectively, confirming the relation $N(D,\alpha) = N_0(\alpha) \cdot (D/D_0)^{-p}$ (p = 3.5, 5.0, and 4.3 for Cu, Ti, and W, respectively). A power law covering one order of magnitude of diameters points to the involvement of fractal processes. The power law was confirmed for the studied cathode materials Cu, Ti, and W. The number of emitted droplets per arc for W is considerably reduced compared to Cu and Ti.
- The discovered relations between the particle diameters and the velocities are of statistical nature and seem to differ for shallow and steep angles, respectively.
- The distribution of emission velocities v_0 peaks for shallow angles ($\alpha < 45°$). Both, the mean velocities $\langle v_0 \rangle$ and the widths σ_v of the distributions decline with rising diameter D of the particle. A power law $\langle v_0 \rangle \sim D^{-k}$ could be fitted (k = 1.46, 1.37, and 1.82 for Cu, Ti, and W, respectively). For the same diameters, the velocities are the highest for Ti, somewhat smaller for Cu, and only half for W.
- At steep angles ($\alpha > 45°$), the data decompose into two groups with no clear relation between D and $\langle v_0 \rangle$. For Cu slow particles concentrate at about 25 m/s, and faster particles at about 70 m/s. An extrapolation of the velocity dependence predicts large velocities (≈ 150 m/s) for small particles (D < 1 µm). The presented data are generally consistent with studies reported in the literature.
- On many occasions, peaks were registered from particles that accidentally underwent reflections at different parts of the vessel, rejected by the verification process. Only those suffering an inelastic reflection at the roof flange of the vessel were investigated further. They retrieve typically only one-third of their impact velocity.

The results can be used as input for the simulation of the interaction of particles with the edge plasma of fusion devices. Experiments using other materials (especially refractory metals and stainless steels composites) are planned to get more data relevant for fusion applications.

REFERENCES

[1] A. Anders, "Cathodic Arcs: From Fractal Spots to Energetic Condensation", in Springer Series on Atomic, Optical, and Plasma Physics, 50, New York, 2008, Online: https://www.springer.com, e-ISBN: 978-0-79108-1.

[2] J.E. Daalder, J. C. A. M. Gordens, "Velocities of macroparticles generated in the cathode spot region of a vacuum arc", *Proc. XVIth ICPIG*, Düsseldorf, pp. 274-275, 1983.

[3] S. Shalev, R. L. Boxman, S. Goldsmith, “Macroparticle dynamics during multi-cathode spot vacuum arcs”, *IEEE Trans. Plasma Sci.* PS-14, no.1, pp. 59-62, 1986.

[4] T. Schülke, and A. Anders, “Velocity distribution of carbon macroparticles generated by pulsed vacuum arcs*”, Plasma Sources Sci. Technol.*, vol. 8, pp. 567-571, 1999.

[5] J.E. Daalder, “Cathode erosion of metal vapour arcs in vacuum”, Thesis, Eindhoven University of Technology, Eindhoven, The Netherlands, 1978.

[6] T. Utsumi, J. H. English, “Study of electrode products emitted by vacuum arcs in form of molten metal particles”, *J. Appl. Phys.*, vol. 46, no. 1, pp.126-131, 1975. DOI: 10.1063/1.321333.

[7] D.T. Tuma, C.L. Chen, D.K. Davies, “Erosion products from the cathode spot region of a copper vacuum arc”, *J. Appl. Phys.*, vol. 49, no.7, pp. 3821-3831, 1978.

[8] G. Distatnik, R.L. Boxman, S. Goldsmith, “Characteristics of Macro-particle Emission from a High Current Density Multi-cathode-spot Vacuum Arc”, *IEEE Trans. Plasma Sci.* PS-15, no. 5, pp. 520-523, 1987.

[9] A. Anders, “Growth and decay of macroparticles: A feasible approach to clean vacuum arc plasmas?“, *J. Appl. Phys.* Vol. 82, pp. 3679-3688, 1997. DOI: 10.1063/1.365731.

[10] D.I. Proskurovsky, S.A. Popov, A.V. Kozyrev, E.L. Pryadko, A.V. Batrakov, and A.N. Shishkov, “Droplets Evaporation in Vacuum Arc Plasma”, *IEEE Trans. Plasma Sci.*, vol.35, no.4, pp. 980-985, 2007.

[11] S. Anders, A. Anders, K. M. Yu, X. Y. Yao, I. G. Brown, “On the macroparticle flux from vacuum arc cathode spots“, *IEEE Trans. Plasma Sci.*, vol.21, no.5, pp .440-446, 1993.

[12] P. Siemroth, T. Schülke, and T. Witke, “High-current arc - a new source for high-rate deposition”, *Surf. Coat. Technol.* vol. 68, pp. 314–319, 1994.

[13] I.I. Aksenov, A.A. Andreev, V.A. Belous, V.E. Strelnickij, and V.M. Khoroshikh, “Vacuum arc: sources of plasma, coating deposition, surface modification”, Publisher: Naukowa Dumka, Kiev, Ukraine, 2012. ISBN 978-966-00-1134-2.

[14] M. Laux, M. Balden, and P. Siemroth, “Modification of arc emitted W-particles in the scrape-off layer plasma”, *Phys. Scr.*, Volume 2014, Number T159, 2014. DOI:10.1088/0031-8949/2014/T159/014026.

[15] V. Rohde, M. Balden, R. Neu, and the ASDEX Upgrade Team, “Arc behaviour on different materials in ASDEX Upgrade”, *Nuclear Materials and Energy*, vol. 29, 101083, 2021. https://doi.org/10.1016/j.nme.2021.101083

[16] H. T. C. Kaufmann, M. D. Cunha, M. S. Benilov, W. Hartmann and N. Wenzel, “Detailed numerical simulation of cathode spots in vacuum arcs: Interplay of different mechanisms and ejection of droplets”, *J. Appl. Phys.*, vol. 122, no. 16, pp. 163303, 2017.

[17] L. Vignitchouk, A. Khodak, S. Ratynskaia, I.D. Kaganovich, “Numerical benchmark of transient pressure-driven metallic melt flows”, *Nuclear Materials and Energy*, vol. 25, 100826, 2020, https://doi.org/10.1016/j.nme.2020.100826.

[18] Lijun Wang, Xiao Zhang, Jiagang Li, Ming Luo, and Shenli Jia, “Study of cathode-spot crater and droplet formation in a vacuum arc”, *J. Phys. D: Appl. Phys.*, vol. 54, 215202 (13pp), 2021.

[19] P. Siemroth, M. Laux, H. Pursch, J. Sachtleben, M. Balden, V. Rohde, and R. Neu, “Diameters and velocities of droplets emitted from the Cu cathode of a vacuum arc”, *IEEE Trans. Plasma Sci*. PS-47, no. 8, pp. 3470-3477, 2019.

[20] P. Siemroth, M. Laux, H. Pursch, J. Sachtleben, M. Balden, V. Rohde, and R. Neu, “Properties of Droplets Emitted from Vacuum Arc Cathodes Made of Copper, Tungsten and Titanium”, *Proceedings XXIX Int. Symp. on Discharges and Electrical Insulation in Vacuum* – Padova, pp. 206-209, 2020, DOI: 10.1109/ISDEIV46977.2021.9587256.

Peter Siemroth was born in Berlin Germany on May 11, 1948. He received the Dipl. Phys. degree 1973 from the Moscow Lomonossov University and the doctorate degree from the Academy of Sciences of the GDR. From 1973 until 1989, he was with the Central Institute of Electron Physics in Berlin. In 1990, he joined the Fraunhofer Institute for Materials Physics and Surface Eng. (IWS) in Dresden. In 2003, he was one of the founders and since then director of the enterprise "Arc Precision GmbH", until its winding-up in 2018. His main research interests are in the investigation of vacuum arc processes and in various applications of arc discharges.

Michael Laux was born in 1948 in Schwerin, Germany. He received his first degree and his PhD in theoretical solid state physics from the Technical University, Dresden. Since 1974, he was with the plasma and surface science department of the Central Institute of Electron Physics. He spent work stays at the Kurchatov Institute, Moscow, the JET project, Abingdon, and the Forschungszentrum Jülich working on plasma surface interaction in fusion devices. Since 1992, he worked for the Max-Planck-Institute of Plasma Physics, Garching, on the field of divertor physics and from 2003 until his retirement for the W7-X project, Greifswald.

Heinz Pursch was born in 1953. He received the M.S. degree from Humboldt-University, Berlin, Germany, in 1976 and the PhD from the Academy of Sciences, Berlin, in 1985. From 1976 to 1991, he was with the former Central Institute of Electron Physics, Berlin, where he was involved in vacuum arc research and current interruption phenomena. During 1992, he was with the Institute of Welding Technology of the Technical University of Braunschweig where he studied physical processes at welding electrodes. From 1993 to 1999, he was with the research group „Electrode Processes” at the Institute of Physics, Humboldt-University Berlin and engaged in research on vacuum arcs and high-pressure discharges. From 2000 to 2001, he has been working at the Institute of Low Temperature Plasma Physics in Greifswald. From 2001 to 2016, he was with Eaton Industries GmbH in Bonn where he was involved in research related to circuit breaker development.

Jürgen Sachtleben was born in Roitzsch, Germany, in 1950. He received the degree in physics from Ernst-Moritz-Arndt-University Greifswald in 1973. In 1982, he obtained a second degree in microprocessor technology from Technical University Dresden. From 1978 to 2013, he was the head of the electronics R&D department at the Max-Planck-Institut for Plasma Physics, Subdivision Greifswald.

Martin Balden got his Diploma (Physics) from the Technical University of Aachen (RWTH) in 1992. His PhD-work was on hydrogen absorption on tungsten (110) made at the Forschungszentrum Jülich, Germany. In 1996, he received the Dr. rer. nat. (Physics) at Technical University of Aachen (RWTH). Since 1996, he works as a scientist at the Max-Planck-Institut für Plasmaphysik, Garching, Germany, with the research focused on material characterisation, especially scanning electron microscopy, mainly on carbon and tungsten-based materials and on samples exposed to fusion plasmas.

Volker Rohde was born on 19th of February 1961, in Preetz, Germany. He received his Dr. rer. nat. degree in plasma physics from the Christian Albrechts University, Kiel in 1993. In 1993, he took up a Postdoc position at the Max-Planck-Institut für Plasmaphysik (IPP) in Berlin, Germany, and in 1997, he changed to Garching. He is responsible for vacuum systems and wall conditioning at the tokamak experiment ASDEX Upgrade. His research focus is on plasma wall interaction, neutral gas analysis and erosion processes.

Rudolf Neu was born on 28th of June 1961, in Tübingen, Germany. He received his Dr. rer. nat. degree in nuclear physics from the University of Tübingen in 1992. 2011, he was appointed associate professor at the University of Tübingen and January 2014 he was appointed as professor for plasma material interaction at the Technical University of Munich. In 1992, he took up a Postdoc position at the Max-Planck-Institut für Plasmaphysik (IPP) in Garching, Germany, and in 2006, he was appointed Group Head. During 2012 – 2013, he was head of the ITER physics department of the European Fusion Development Agreement (EFDA) and from 2014, on he returned to IPP as a Group Head and leader of the plasma wall interaction activities. Also, in 2014 he became editor of the journal 'Fusion Engineering and Design'(Elsevier) and was selected for the ISI list of 'Highly Cited Researchers' in the category 'Engineering'.